This manuscript was accepted by Appl. Phys. Lett. Click here to see the version of record.

Electrical and magnetic properties of hemozoin nanocrystals

M. Giacometti[1], C. Rinaldi[2,3], M. Monticelli[2], L. Callegari[2], A. Collovini[1], D. Petti[2], G. Ferrari[1], R. Bertacco[2,3]

[1] Dipartimento di Elettronica, Informazione e Bioingegneria, Politecnico di Milano, Via Giuseppe Colombo 81, 20133 Milan, Italy

[2] Dipartimento di Fisica, Politecnico di Milano, Via Giuseppe Colombo 81, 20133 Milan, Italy

[3] IFN-CNR, c/o Politecnico di Milano, Piazza Leonardo da Vinci, 32, 20133 Milano, Italy.

Abstract

Hemozoin crystals, also known as malaria pigment, are the by-product of hemoglobin degradation by the Plasmodium parasite during its intra-erythrocytic development. Although it is well known that they are responsible for the peculiar paramagnetic behavior of infected red blood cells, their physical properties are not well known. Here we show that synthetic hemozoin nanocrystals display an insulating and paramagnetic behavior. Conductive atomic force microscopy measurements on crystal dispensed over flat Au films reveal that hemozoin crystals are insulating, with a breakdown field larger than $5 \cdot 10^7$ Vm^{-1}. The magnetic susceptibility, measured with a vibrating sample magnetometer, is $4.1 \pm 0.6 \cdot 10^{-4}$, compatible with a paramagnetic behavior. These results are confirmed by impedimetric and magnetophoretic mesurements on aqueous suspensions of hemozoin crystals.

This manuscript was accepted by Appl. Phys. Lett. Click here to see the version of record.

Text

According to World Health Organization, 3.2 billion people are at risk for malaria. In 2016, 216 million new cases occurred and 445000 deaths have been estimated.[1] Although treatment in the early stage of the disease is usually very effective, the on-site early diagnosis is still an open issue. Conventional tests via optical microscopy examination of blood smears take about one hour and need skilled microscopists, while rapid diagnostic tests (RDT) are prone to a large percentage of false positives, as they are based on the detection of antigens which can be hardly washed out in a patient living in an endemic zone. This leads to improper treatment of patients not really affected by malaria, thus increasing the risk of drug resistance.[2,3] In this scenario, there is a strong need of novel RDTs with (i) the same sensitivity of the gold standard (optical microscopy examination) and (ii) a reduced number of false positives.[1,4,5] To fulfill the last requirement, a real improvement would be to move back to the quantification of infected red blood cells (i-RBC) in a blood smear, like in gold standard tests, with the additional requirement of integrating i-RBC counting in lab-on-chip platforms suitable for low-cost, rapid and on-site wide screening of the population in endemic zones.

It is well known that i-RBCs display a paramagnetic behavior with respect to blood plasma, so that a high magnetic field gradient can be used to separate them from healthy ones.[3,6,7,8] On the other hand, the manipulation and detection of magnetic particles on-chip has achieved a good maturity[9,10] and hold potential for the integration of magnetophoretic based detection of i-RBC. The origin of RBC paramagnetism is connected to the degradation of hemoglobin into free heme, during the Plasmodium parasite intra-erythrocytic development. This molecule, highly toxic to the parasite, is converted in an insoluble form, known as hemozoin, which crystallizes into paramagnetic nanocrystals found both within the i-RBCs and free in the blood, after RBCs lysis.[11,12] Although HC can be produced also by blood-feeders parasites other than Plasmodium,[13,14] they are of overwhelming relevance for malaria diagnostics, as they constitute the characteristic malaria pigment allowing for the recognition of i-RBC by optical microscopy investigation. More recently, malaria detection schemes have been proposed which exploit the magnetic and optical properties of HC.[15,16, 17,18] Nevertheless the physical

This manuscript was accepted by Appl. Phys. Lett. Click here to see the version of record.

properties of hemozoin are still poorly understood. While their magneto-optical properties have been widely investigated, a reliable and unambiguous evaluation of fundamental quantities like the electrical conductivity and magnetic susceptibility is still missing. In literature there are no data on the electrical properties of hemozoin crystals, both under constant (DC) and alternating (AC) bias, apart from some preliminary electrical measurements on aqueous suspensions of HC[19] and very recent cyclic voltammetry results.[20] It is not evident at all whether HC display an insulating or conductive behavior at low bias, where electrochemical reactions are not activated, while this information would be crucial for the development of impedimetric detection schemes. Coming to magnetism, while some papers report a paramagnetic behavior of HC, with values of the susceptibility on the order of $3.2 \cdot 10^{-4}$,[21,22] a superparamagnetic behavior has been suggested in a more recent paper by Inyushin et al.,[23,24] corresponding to a susceptibility larger than 10^3.

To shed light on these subjects, we have investigated synthetic HC, i.e. β-hematin crystals provided by Invivogen, the very same crystals used by Inyushin et al. in their paper. These nanocrystals represent a good model for natural hemozoin produced by Plasmodium, displaying the same properties and similar size distribution.[25,12,26] Their positive magnetic susceptibility is due to the transformation of the low-spin (4 μ_B) Fe^{2+} ions present in diamagnetic oxyhemoglobin into Fe^{3+} high-spin (5 μ_B) ions.[17] According to X-ray diffraction data, hemozoin or β-hematin crystals are made of chains of dimers of Fe^{III}-protoporphirin–IX molecules, also called heme monomers, linked by hydrogen bonds. In each dimer, the Fe^{III} ion, located at the center of the porphyrin ring, 0.47 Å above the porphyrin plane, is bound to four nitrogen atoms of the same porphyrin and to one of the oxygens of the protoporphyrin-IX propionic acid substituents belonging to the other Fe^{III}-protoporphirin–IX molecule. The distance between the Fe^{III} ions in the same dimer is 9.05 Å, while that between nearest Fe^{III} ions neighbors in adjacent dimers is 7.86, 8.04 and 8.07 Å.[14,27]

The electrical characterization by current sensing atomic force microscopy (CS-AFM) has been carried out on HC placed on a conductive substrate. To this scope, we dispensed a few drops of a

This manuscript was accepted by Appl. Phys. Lett. Click here to see the version of record.

suspension of HC in DI water on a 100 nm thick Au film deposited on a Si(001) substrate and we waited for water evaporation before starting measurements. The crystals display a typical brick-like shape, with lateral size of about 200-300 nm and length lower than 1 μm, as seen by scanning electron microscopy (SEM) and AFM. CS-AFM was performed using a conductive Pt-Ir coated n-doped silicon tip by Applied NanoStructures Inc. (AppNano ANSCM-PT, L= 225 μm, k= 3 N/m). We applied the whole range of available voltage bias (-10 V, +10 V) and the current was recorded by using the AFM transimpedance current pre-amplifier. First, local I-V curves were collected over a mesh of points on the sample surface, to avoid the wear-off of the conducting coating of the tip. Then, the topography was acquired in contact mode to associate I-V curves either to hemozoin or gold. Figure 1a reports an example of sample morphology, with some clusters of HC on the flat Au surface. Two representative I-V curve collected on Au (orange dot in panel a) and on a single HC (blue dot in panel a) are reported in Figure 1b. A radically different behavior is found on hemozoin and gold. On the Au film the saturation of the current amplifier (10 nA) is reached already at 1 mV bias, corresponding to a total impedance lower than 10^5 Ω, including the tip resistance (R_T ~ 1 kΩ according to provider specifications), the tip-film resistance (R_{TF}) and the Au film resistance (R_{Au}) towards the lateral electric contact. On the HC crystal, instead, the tip current remains below 10 pA up to the maximum applied voltage. The total equivalent resistance at 10 V is 10^{12} Ω, while the breakdown field is larger than $5 \cdot 10^7$ V·m^{-1}, by assuming a crystal thickness at the point of measurement of about 200 nm, as resulting from the AFM topography. A similar behavior was observed for all the hemozoin crystals investigated. Even though a quantitative estimate of the hemozoin bulk resistivity is prevented by the uncertainty on the tip-HC and HC-Au contact resistance, our results indicate a clear DC insulating behavior.

To investigate the AC electrical beahvior up to the frequency region of interest for impedimetric measurements in liquid, typically in the MHz range, we directly measured the change of the impedance between interdigitated Au electrodes immersed in a suspension of HC in a Phosphate Buffer Solution (1x Dulbecco's PBS), upon sedimentation of HC crystals. The electrodes, 100 nm

This manuscript was accepted by Appl. Phys. Lett. Click here to see the version of record.

high, 2 μm wide and separated by 2 μm (see inset of Figure 2a), were micro-fabricated by optical lithography and lift-off on a glass substrate. The magnitude of the complex impedance Z of the interdigitated electrodes immersed in PBS is plotted in Figure 2a as a function of frequency. At low and high frequency, a capacitive behavior is expected, due to the double layer capacitance (C_{dl}) and geometrical capacitance of the electrodes (C_{el}), respectively.[28] In between, there is a frequency region where a resistive behavior is observed, dominated by the resistance of the solution (R_{sol}) above the electrodes. This corresponds to the flat portion of the curve in Figure 2a, above 1 MHz, following the low frequency region dominated by C_{dl}. The effect of the geometrical capacitance is not seen, as it would be at higher frequency, where inductive parasitic effects prevent a reliable measurement.

Based on this characterization, we performed impedimetric experiments at 3 MHz, where measurements are more sensitive to HC just above the electrodes. The resistive term of the impedance, i.e. the real part, was monitored vs. time, to further reduce the effects of spurious capacitive and inductive terms. In Figure 2b, we report the normalized resistance change ($\Delta R/R$) measured during the sedimentation of HC suspended in PBS at different concentrations: 0.01 mg/ml (C1), 0.03 mg/ml (C2), 0.06 mg/ml (C3). The resistance increases over time, thus indicating that the probing volume above the electrodes is gradually occupied by particles (see panels c, d, e in Figure 2) with resistivity higher than that of the PBS medium. We estimated the volumetric fraction occupied by HC at the end of the experiments, defined as the volume of HC crystals in the probing volume of the electrodes normalized to said probing volume, from the images of Figure 2. To this scope, we evaluated the ratio of the black areas (upon subtraction of the area of the black lines corresponding to the interstitial regions between the electrodes) with respect to the total area of the electrodes (white regions). This can be assumed as representative of the fraction of the electrode surface occupied by HC: A_{HC}/A_{el}. By numerical simulations the probing volume was estimated to be the electrode area multiplied by a probing depth corresponding to about 1.5 times the electrodes spacing. Assuming that, at low concentrations, we have a single layer of HC (250 nm high, compatible with AFM and SEM images) the volumetric fraction (ϕ) is given by the following equation: $\phi = A_{HC}/A_{el} \cdot (0.25/3)$.[28]

This manuscript was accepted by Appl. Phys. Lett. Click here to see the version of record.

Finally, the expected percentage of resistance variation (ΔR/R) in case of insulating particles is estimated according to Maxwell's mixture theory assuming an insulating behavior of HC: $\Delta R/R = 3/2 \cdot \phi$.

In Table I we report the experimental ΔR/R for the asymptotic situations in panels 2c, 2d, 2e, corresponding to HC concentrations C1, C2 and C3, together with the ΔR/R estimated as described above.

HC concentration C (mg/ml)	ΔR/R (%) experimental	ΔR/R (%) estimated
C1 = 0.01	1.8 ± 0.2	2.0 ± 0.25
C2 = 0.03	2.9 ± 0.3	3.6 ± 0.5
C3 = 0.06	6.2 ± 0.5	6.0 ± 0.5

Table I: Experimental and estimated percentage variation of the resistance as a function of the concentration of hemozoin crystals.

The good agreement between experimental and estimated values, for different HC concentrations, confirms the validity of the assumption that HC are insulating also in the MHz frequency range and points to the possibility of using ΔR/R to evaluate the volumetric fraction of HC on top of interdigitated electrodes.

The magnetic properties of synthetic HC by Invivogen have been investigated by using a Vibrating Sample Magnetometer (Microsense EZ9), with sensitivity down to 10^{-9} A·m^{-1}. The biggest ball of crystals in the glass container used for shipment has been directly used for measurements, without suspending it in any solution, as in Ref. 23. Its mass, 3.3±0.2 mg, has been determined with a

This manuscript was accepted by Appl. Phys. Lett. Click here to see the version of record.

microbalance, after insertion in the VSM cuvette. The magnetic moment has been then measured when sweeping the external field $\mu_0 H$ from -1.5 to +1.5 T. The corresponding hemozoin magnetization curve $M(\mu_0 H)$, plotted in Figure 3a, has been obtained after subtraction of the diamagnetic background from the cuvette and normalization to the hemozoin sample volume. The latter has been estimated from the mass of the ball, using a tabulated value for the hemozoin density: $\rho_{HC} = 1.49\ g \cdot cm^{-3}$. The linear trend over the whole investigated magnetic field range, with positive angular coefficient, clearly indicates a paramagnetic behavior, with magnetic susceptibility $\chi = M/H = 3.5 \pm 0.2 \cdot 10^{-4}$ in SI units. This value is very close to that calculated by Coronado et al.,[22] $\chi = 3.20 \cdot 10^{-4}$, starting from the experimental results acquired by Hackett et al.[21]

On the other hand, at variance with the paper by Inyushin et al.,[23] there is no trace of superparamagnetic behavior. To confirm the reliability of our results, a second batch of synthetic hemozoin crystals provided by Invivogen has been tested. The measured value of the susceptibility was $4.7 \pm 0.4 \cdot 10^{-4}$, in nice agreement with the previous one. The average value of the two measurements is $4.1 \cdot 10^{-4}$, with an error bar on the order of $\pm 0.6 \cdot 10^{-4}$, probably arising from the variability of sample preparation procedures.

The absence of superparamagnetic behavior has been checked also in independent experiments of sedimentation assisted by an external magnetic field. We used an array of interdigitated electrodes with a permanent magnet underneath and we monitored the evolution of the electrodes resistance at 3 MHz, upon dispensation of a suspension of HC and superparamagnetic beads (1 μm Dynabeads® MyOne™ Carboxylic Acid) in PBS. The number of interdigitated fingers was 20; their length, width and spacing were 400, 2 and 2 μm, respectively. The electrodes were fabricated on a 500 μm thick glass substrate, with a PDMS well on top (2 mm high) for the dispensation of the particle suspension. A cylindrical NdFeB magnet was placed in contact with the bottom surface of the chip, producing an out-of-plane magnetic field H with an average strength and gradient

This manuscript was accepted by Appl. Phys. Lett. Click here to see the version of record.

component along the out-of-plane (z) direction of $1.3 \cdot 10^5$ A·m^{-1} and $1.2 \cdot 10^8$ A·m^{-2}, respectively, over the 2 mm of the suspension in the well.

We choose beads of size and density (ρ_b = 1.8 g·cm^{-3}) comparable to those of HC, to work in similar conditions of Brownian motion and drug forces acting on the particles during the magnetically assisted sedimentation. The impedance variation vs. time is reported in Figure 3b for HC and superparamagnetic beads. We observe a much faster sedimentation (at least by a factor 50) for superparamagnetic beads with nominal susceptibility of the order of unity, according to technical specification from the provider. This behavior is in qualitative agreement with the estimated sedimentation times for superparamagnetic beads and paramagnetic HC, while it could not be explained by assuming that HC are superparamagnetic. The establishment of the equilibrium concentration in a magnetic suspension with height L can be dominated either by diffusion or by sedimentation under the action of a uniform external force, depending on the ratio L/l, where l = k_BT/F is a characteristic length of the process.[29,30] For L>>l, as in the present case, sedimentation under the action of gravity, buoyancy and magnetic force, is the dominant factor, giving rise to a characteristic sedimentation time $\tau_s \sim Ll/D$, where $D = k_BT/6\pi\eta a$ is the diffusion coefficient, η the viscosity and a the particle radius. The total average force (F_b) acting on MyOne beads has been estimated according to the following equation:

$$F_b = (\rho_b - \rho_l)V_b g + \mu_0 V_b (M \cdot \nabla)H \qquad (1)$$

where ρ_l = 1 g·cm^{-3} is the density of PBS, V_b the bead volume, g the acceleration of gravity, μ_0 the vacuum permeability; M = $4.3 \cdot 10^4$ A·m^{-1} is the bead magnetization in the average magnetic field produced by the magnet over the height of the well according to the particle data sheet, $\nabla H = 1.2 \cdot 10^8$ A·m^{-2} is the average value for the z component of the gradient of the magnetic field H.

The total average force (F_{HC}) acting on HC is given by equation (2), where the magnetic force has been evaluated considering that in this case the susceptibility is constant up to 1.5 T:

This manuscript was accepted by Appl. Phys. Lett. Click here to see the version of record.

$$F_b = (\rho_{HC} - \rho_l)V_{HC}g + \frac{1}{2}\mu_0 V_{HC}\chi\nabla H^2 \quad (2)$$

where $V_{HC} = 6.2 \cdot 10^{-20}$ m^3 is the volume of a single hemozoin crystal assuming a parallelepiped shape with sides of 0.25, 0.25 and 1 μm, $\nabla H^2 = 6.8 \cdot 10^{13}$ A^2·m^{-3} is the average value over the well height for the z component of the gradient of H^2.

With these values, using the average magnetic forces of equations (1) and (2) to apply the model by Raikher et al.,[30] we calculated the expected sedimentation times for MyOne beads and HC, treated as spherical particles, which turn out to be $\tau_{sb} \sim 7$ s and $\tau_{sHC} \sim 7500$ s. Despite the quite crude approximations used in the model, the order of magnitude is coherent with the experimental sedimentation times seen in Figure 3. On the other hand, assuming a superparamagnetic behavior as that reported by Inyushin et al.[23], the magnetic force on HC would be 4 orders of magnitude larger than that expected from our VSM measurements, and, consequently, the estimated sedimentation time would decrease down to 2 s. Clearly this is not compatible with experimental data presented in Figure 3b, thus confirming that HC do not display a superparamagnetic behavior.

This is not completely surprising because the direct exchange interaction mechanism between Fe^{3+} ions in HC is negligible, due to the large distance (7.86 Å) between nearest neighbors in adjacent unit cells made of heme dimers.[27] Furthermore, multi-frequency high-field electron paramagnetic resonance measurements allow to exclude a sizable exchange coupling mediated by d-π orbital overlap, like that observed in linear copper porphyrin oligomers.[31] In absence of a sizable exchange coupling, Fe^{3+} ions just behave as paramagnetic spin centers, as confirmed also by independent magnetometry and magneto-optical analysis of HC.[17]

To summarize, in this paper we report on the electrical and magnetic characterization of synthetic hemozoin or β-hematin nano-crystals. They behave as insulating particles, both in DC and at 3 MHz.

On the other hand, independent magnetometry and magnetophoretic experiments confirm their paramagnetic behavior, with magnetic susceptibility at room temperature of $4.1\pm0.6\cdot10^{-4}$. Even though we do not find trace of superparamagnetic behavior, the susceptibility value is not negligible and suitable for magnetophoretic capture. These results set the proper framework for the development of malaria diagnostic tests based on magnetophoretic capture and impedimetric detection of hemozoin crystals in blood samples.

Acknowledgments

We thank M. Sampietro, G.B. Fiore, E. Giuliani, F. Milesi and G. Bussetti for fruitful discussions and assistance during experiments. This work was supported by Politecnico di Milano, under project Tid-Mekii (Polisocial Awards 2016), and has been mainly carried out at Polifab, the micro and nanofabrication facility of Politecnico di Milano.

REFERENCES

1. World Health Organization, World malaria report 2017. (2017).
2. Moody, A. Clinical Microbiology Reviews, 15, 66–78 (2002).
3. Kasetsirikul, S., Buranapong, J., Srituravanich, W., Kaewthamasorn, M. & Pimpin, A. Malar. J. 15, 358 (2016).
4. Roberts, B. L., Science, 352 (6284), 398-405 (2016).
5. Grimberg, B. T. & Grimberg, K. O. Expert Rev Anti Infect Ther. 14(10): 879–883 (2016)
6. Zimmerman, P. A., Thomson, J. M., Fujioka, H. & Collins, W. E. MICROSCOPY. 74, 568–572 (2013).
7. Ribaut, C., Berry, A., Chevalley, S., Reybier, K., Morlais, I., Parzy, D., Nepveu, F., Benoit-Vical, F. and Valentin, A., Malaria Journal. 1–5 (2008).
8. Han, K., Frazier, A. B., J. Appl. Phys. 96(10), 5797, (2004).

9. Donolato, M., Vavassori, P., Gobbi, M., Deryabina, M., Hansen, M. F., Metlushko, V., Ilic, B., Cantoni, M., Petti, D., Brivio, S. and Bertacco, R., Advanced Materials, 22, 2706–2710 (2010)

10. Torti, A., Mondiali, V., Cattoni, A., Donolato, M., Albisetti, E., Haghiri-Gosnet, A. M. , Vavassori, P. and Bertacco, R. Appl. Phys. Lett. 101, 142405 (2012).

11. Hänscheid, T., Egan, T. J. & Grobusch, M. P. Lancet Infectious Diseases 7, 675–685 (2007).

12. Noland, G. S., Briones, N. & Jr, D. J. S. Molecular and Biochemical Parasitology 130, 91–99 (2003).

13. Lvova, M., Zhukova, M., Kiseleva, E., Mayboroda, O., Hensbergen, P., Kizilova, E., Ogienko, A., Besprozvannykh, V., Sripa, B., Katokhin, A., Mordvinov, V., International Journal for Parasitology 46, 147–156 (2016).

14. Egan, T. J. Journal of Inorganic Biochemistry 102, 1288–1299 (2008)

15. Newman, D. M., Heptinstall, J., Matelon, R. J., Savage, L., Lesley Wears, M. , Beddow, J., Cox, M., Schallig, Henk D. F. H. and Mens, Petra F., Biophysical Journal 95, 994–1000 (2008).

16. Kim, W., Ozdemir, S. K., Zhu, J., Monifi, F. & Yang, L., Optics Express, Vol. 20, No. 28, 29426 (2012)

17. Butykai1, A., Orban, A., Kocsis, V., Szaller, D., Bordacs, S., Tatrai-Szekeres, E., Kiss, L. F., Bota, A., Ve´rtessy, G. B., Zelles, T., Kézsmarki, I., Scientific Reports, 3:1431 (2013)

18. Pirnstill, C. W. & Coté, G. L. Scientific Reports 5, (2015)

19. Paula, N., PhD dissertation (2014).

20. Hyeon, J.E., Jeong, D.W., Ko, Y.J., Kim, S.W., Park, C., Han, S.O.. Biosensors and Bioelectronics, 114, 1–9 (2018).

21. Hackett, S., Hamzah, J., Davis, T. M. E. & St Pierre, T. G. Biochim. Biophys. Acta - Mol. Basis Dis. 1792, 93–99 (2009).

22. Coronado, L. M., Nadovich, C. T. & Spadafora, C. Biochim. Biophys. Acta - Gen. Subj.

1840, 2032–2041 (2014).

23. Inyushin, M., Kucheryavih, Yu., Kucheryavih, L., Rojas, L., Khmelinskii, I. , Makarov, V. , Scientific Reports, 6:26212 (2016).

24. Khmelinskii, I. & Makarov, V., Chem. Phys. 493, 120–132 (2017).

25. Pagola, S., Stephens, P. W., Bohle, D. S., Kosar, A. D. & Madsen, S. K. Nature, 404, 307–310 (2000).

26. Dilanian, R.A., Streltsov, V., Coughlan, H.D., Quiney, H.M., Martin, A.V., Klonis, N., Dogovski, C., Boutet, S., Messerschmidt, M., Williams, G.J., Williams, S., Phillips, N.W., Nugent, K.A., Tilley, L., Abbey, B., J. Appl. Cryst. 50, 1533–1540 (2017).

27. Sienkiewicz, A., Krzystek, J., Vileno, B., Chatain, G., Kosar, A. J., Scott Bohle, D. and Forró, L., J. Am. Chem. Soc. 128, 4534–4535 (2006).

28. Ibrahim, M., Claudel, J., Kourtiche, D. & Nadi, M. J. Electr. Bioimp. 4, 13–22 (2013).

29. Berret, J. F., Sandre, O. & Mauger, A. Langmuir 23, 2993–2999 (2007).

30. Raikher, Y. L. & Shliomis, M. I., J. Magn. Magn. Mater. 122, 93–97 (1993).

31. Richert, S., Kuprov, I., Peeks, M.D., Suturina, E. A., Cremers, J., Anderson, H. L., Timmel, C. R., Phys. Chem. Chem. Phys., 19, 16057 (2017)

Figures captions

Figure 1: (a) Atomic force microscopy image of a few hemozoin crystals over a Au/Si(001) substrate. The blue (orange) dots and arrows represent the point where the local I(V) curves have been measured. (b) I(V) curves measured with the tip in contact with hemozoin (blue) and the bare gold substrate (orange).

Figure 2: (a) Impedance magnitude as a function of frequency for gold interdigitated electrodes (see inset for details) immersed in PBS, without HC. The amplitude of the sinusoidal voltage was 100 mV (b) Normalized impedance change at 3 MHz during sedimentation of HC from suspensions at different concentrations: 0.01 mg/ml (C1), 0.03 mg/ml (C2), 0.06 mg/ml (C3). The error bar for each curve mainly reflects the uncertainty in the subtraction of the baseline and connected drift. (c,d,e) Optical microscopy images of the electrodes with HC at the end of the measurements reported in panel (b) for the concentrations C1, C2 and C3, respectively.

Figure 3: (a) Magnetization vs. applied magnetic field of synthetic hemozoin crystals measured by vibrating sample magnetometry. (b) Normalized impedance variation measured at 3 MHz between interdigitated electrodes immersed in PBS upon magnetically assisted sedimentation of superparamagnetic beads (red line) and hemozoin crystals (blue line).

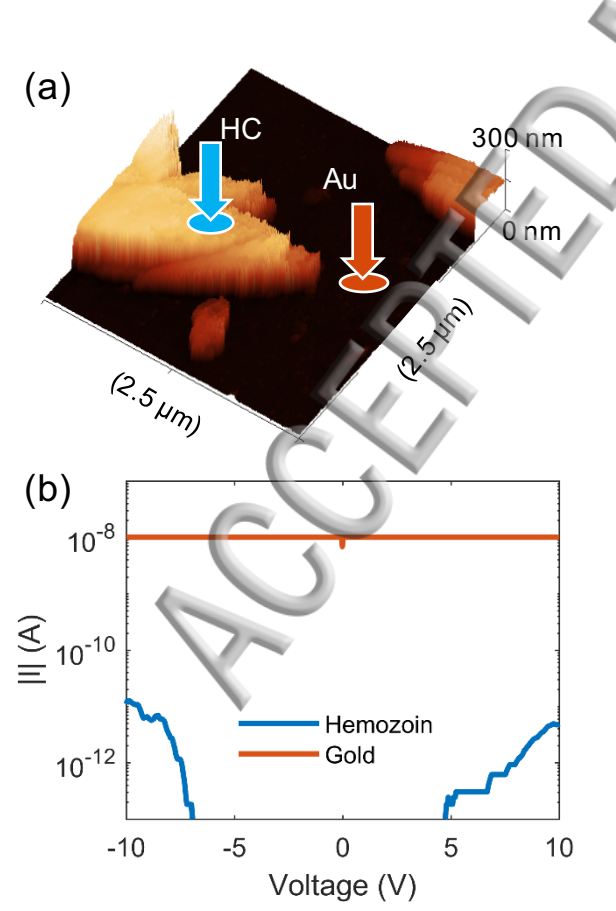

Figure 1

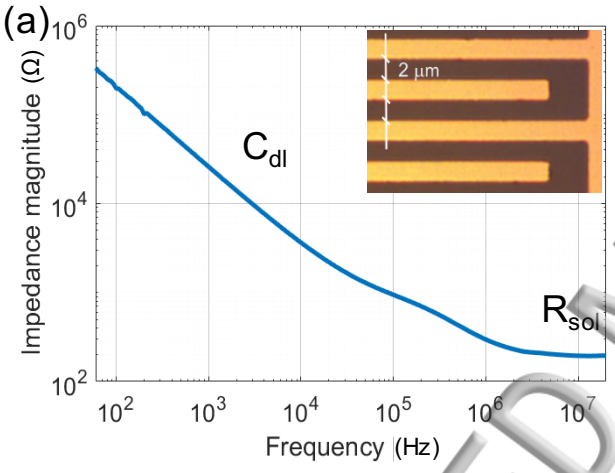

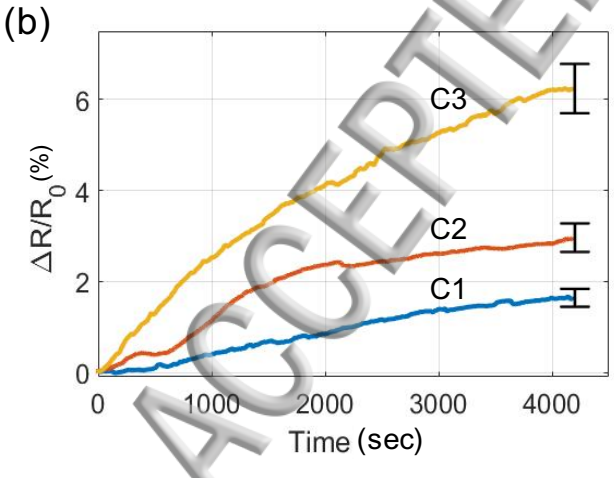

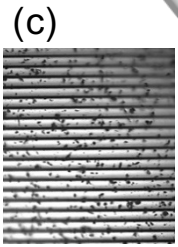

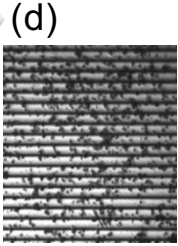

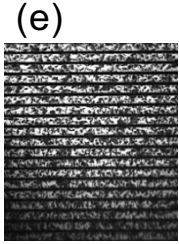

Figure 2

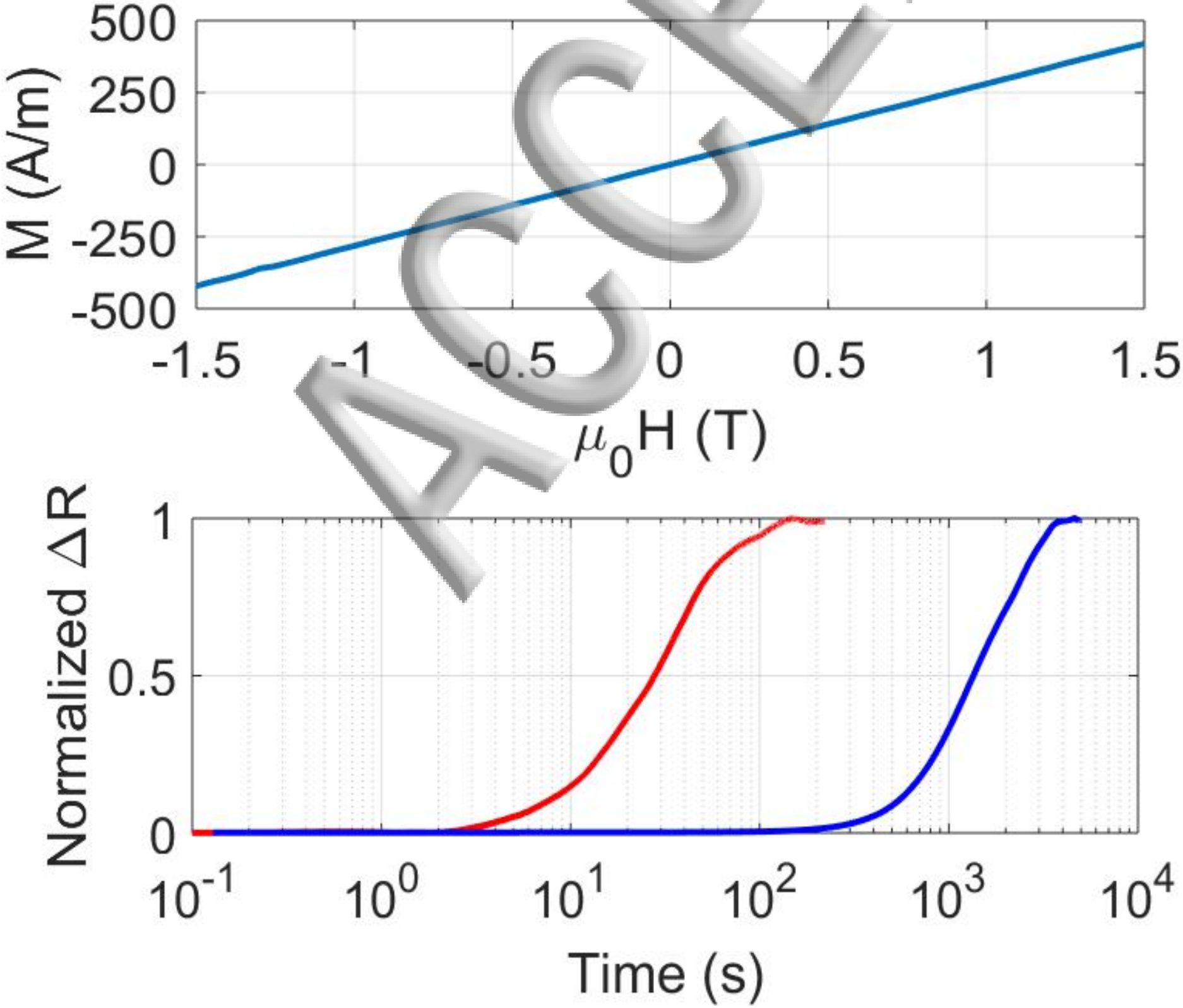

Figure 3